ACS OMEGA

Open Access

http://pubs.acs.org/journal/acsodf

Article

Solid-Phase Extraction at High pH as a Promising Tool for Targeted Isolation of Biologically Active Fractions of Humic Acids

Tatiana A. Mikhnevich, Vitaly G. Grigorenko, Maya Yu. Rubtsova, Gleb D. Rukhovich, Sun Yiming, Anna N. Khreptugova, Kirill V. Zaitsev, and Irina V. Perminova*

Cite This: *ACS Omega* 2024, 9, 1858−1869

Read Online

ACCESS | Metrics & More | Article Recommendations | Supporting Information

ABSTRACT: A search for novel sources of biologically active compounds is at the top of the agenda for biomedical technologies. Natural humic substances (HSs) contain a large variety of different chemotypes, such as condensed tannins, hydrolyzable tannins, terpenoids, lignins, etc. The goal of this work was to develop an efficient separation technique based on solid-phase extraction (SPE) for the isolation of narrow fractions of HS with higher biological activity compared to the initial material. We used lignite humic acid as the parent humic material, which showed moderate inhibition activity toward beta-lactamase TEM 1 and antioxidant activity. We applied two different SPE techniques: the first one was based on a gradient elution with water/methanol mixtures of the humic material sorbed at pH 2, and the second one implied separation by a difference in the pK_a value by the use of sequential sorption of HS at pH from 8 to 3. SPE cartridges Bond Elute PPL (Agilent) were used in the fractionation experiments. The first and second techniques yielded 9 and 7 fractions, respectively. All fractions were characterized using high-resolution mass spectrometry and biological assays, including the determination of beta-lactamase (TEM 1) inhibition activity and antioxidant activity. The acidity-based separation technique demonstrated substantial advantages: it enabled the isolation of components, outcompeting the initial material at the first step of separation (sorption at pH 8). It showed moderate orthogonality in separation with regard to the polarity-based technique. Good perspectives are shown for developing a 2D separation scheme using a combination of polarity and acidity-based approaches to reduce structural heterogeneity of the narrow fractions of HS.

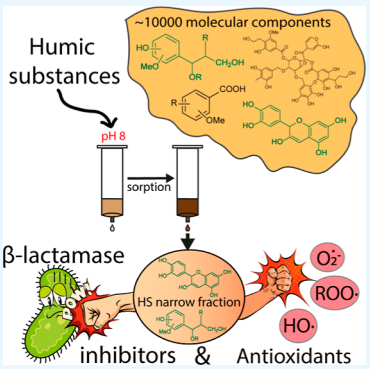

INTRODUCTION

Humic substances (HSs) make up a versatile class of natural compounds with diverse biological activities. HSs are complex supramolecular systems enriched with oxygen-containing carboxylic and phenolic groups, which are formed during the oxidative degradation of biomolecular precursors: lignins, proteins, lipids, polysaccharides, etc.[1,2] The variety of HS molecular composition ensures the expression of antibacterial,[3,4] antiviral,[5−7] antioxidant activities,[8−11] etc. Screening natural product libraries is proposed as a promising approach for discovery of new scaffolds of chemical compounds capable of suppressing the resistance of pathogenic bacteria to antibiotics.[12] Bacterial antibiotic resistance has become as a critical one among the top global health threats.[13,14] It is widespread worldwide, causing millions of deaths due to the ineffectiveness of antibiotics.

Recently, the ability of HS to inhibit serine β-lactamases, which cause the most common resistance of gram-negative bacteria to β-lactam antibiotics, has been demonstrated.[15,16] At the same time, HS are scarcely used in practice due to extreme structural heterogeneity and a high level of isomeric complexity. This complexity can be clearly seen from the data of Fourier transform ion cyclotron mass-spectrometry (FTICR MS) on molecular composition of HS.[17−21] Thanks to the ultrahigh resolution of this technique, several thousand molecular peaks can be determined in a mass spectrum of HS.[21−24] Projection of FTICR MS assignments onto the 2D space of the Van Krevelen diagram makes it possible to visualize the chemical space of HS.[25,26] The presence or absence of certain molecular components on the Van Krevelen diagram is used to relate the structure to the biological activity of HS.[7,27−30] This is due to a lack of efficient techniques for the targeted isolation of individual molecular components from the molecular ensemble of HS.

Fractionation is one of the most effective approaches, which allows for the reduction of chemical and isomeric diversity of HS as well as the extraction of the more biologically active components.[31−35] Solid-phase extraction (SPE) with the use of prepacked cartridges (e.g., Bond Elute PPL) is widely used as a method of preparative extraction of HS from aquatic environments.[36−38] SPE, in combination with gradient elution

Received: October 29, 2023
Revised: December 3, 2023
Accepted: December 5, 2023
Published: December 15, 2023

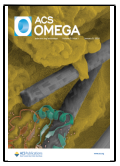

with solvents differing in polarity, was effective in both the separation of molecular components and the isolation of fractions with increased inhibitory activity against β-lactamase TEM.[16,38]

Another version of the SPE technique developed by Zherebker et al.[39,40] applied sequential sorption of HS from solutions with a decreasing pH value, starting with 7. It allows fractions to be obtained with a narrow range of pK_a values. It was shown that the use of HS solutions at pH 7 enabled the isolation of a fraction that was rich in hydrophobic components, such as condensed tannins, lignins, and terpenoids. These components contribute greatly to the biological activity of HS.[41] However, this method has not been used so far at pH values higher than, which are particularly promising for the isolation of more hydrophobic fractions with potentially higher biological activity.

The objective of this study was to compare the efficacy of two different versions of SPE for the targeted extraction of the biologically active components from the humic materials. For this purpose, we used the SPE technique, which implies a gradient decrease in pH starting with pH 8 (SPE-acidity), and the SPE technique based on gradient elution with solvents of different polarities (SPE-polarity) for preparing narrow fractions of HS. We tested the obtained fractions for inhibitory activity against serine β-lactamase (TEM 1) and antioxidant activity.

RESULTS AND DISCUSSION

Fractionation of HS by Polarity and Acidity. According to our previous studies, coal humic acids (CHAs) are the most promising source of β-lactamase inhibitors, unlike humic or fulvic acids of soils and peat.[16] A sample of CHA isolated from commercially available sodium humate "Genesis" (CHA-G) was used in this study. It was characterized by the data on elemental and structural group compositions which are given in the Supporting Information (Table S1).

The SPE separation of CHA-G into narrow fractions by polarity was carried out, as shown in Figure 1a. The humic material was sorbed at pH 2 on the SPE cartridge and then eluted with equal volumes of H_2O/CH_3OH mixtures with an increasing content of methanol in the ratios (vol %): 80:20, 70:30, 50:50, 40:60, 30:70, 20:80, 10:90, 0:100.

For the fractionation of CHA-G by acidity, the SPE method was applied with sequential pH lowering from 8 to 3 (see the Experimental Section and Figure 1b). The molecular components were extracted in the order of affinity for proton binding: at higher pH, the least acidic phenolic components were sorbed, as shown in Figure 1b. The use of this method for HS fractionation required more time and effort in this study compared to the polarity SPE because it implied multiple steps of both sorption and desorption of HS versus the single sorption step of the polarity SPE. The masses of the obtained CHA-G fractions by polarity and acidity are given in Table 1.

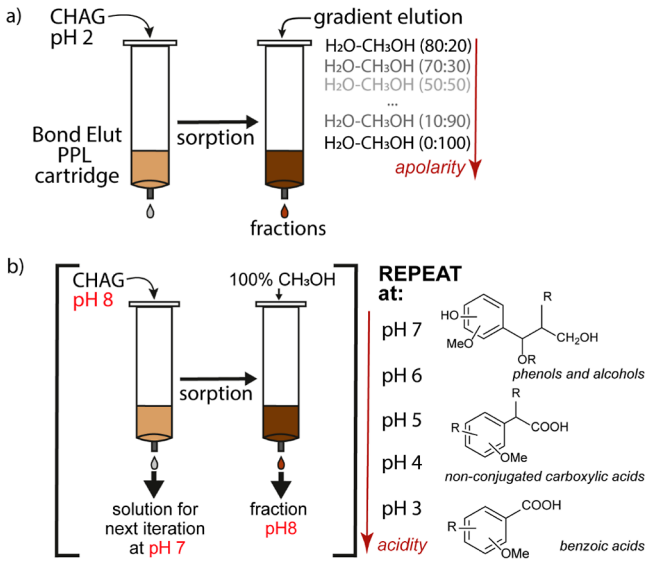

Figure 1. Schemes of isolation of CHA-G narrow fractions (a) by polarity; (b) by acidity.

Table 1. Mass Yields of CHA-G Fractions Obtained by the Two Techniques Used in this Study

by polarity	mass, mg	by acidity	mass, mg
material used for fractionation	355	material used for fractionation	500
CHAG-20	10	CHAG-pH8	18
CHAG-30	2	CHAG-pH7	14
CHAG-50	20	CHAG-pH6	23
CHAG-60	15	CHAG-pH5	21
CHAG-70	17	CHAG-pH4	47
CHAG-80	10	CHAG-pH3	35
CHAG-90	12		
CHAG-100	8		
fractions	94 (26%)	fractions	158 (32%)
irreversibly sorbed material[a]	219 (62%)	irreversibly sorbed material[a]	51 (10%)
non sorbed material[b]	42 (12%)	non sorbed material[b]	291 (58%)

[a]Calculated by subtracting the masses of fractions and unsorbed material from the initial mass. [b]Determined by measurement of UV absorbance of the solution after passing through the cartridge.

It can be seen that a large portion (60%) of the CHA-G sorbed at pH 2 remained on the cartridge even after its elution with 100% methanol (the cartridge maintained a black color). A solvent of higher polarity (e.g., 0.1 M NaOH) was needed to extract the remaining fraction. The opposite situation was observed with the separation by acidity: more than 60% of the initial humic material was not sorbed onto the cartridge at pH 3. It was precipitated by lowering the pH of the final solution until 2. The formed precipitate was composed of very hydrophobic, apolar, resin-like components.

Molecular Compositions of the Narrow HS Fractions Obtained in this Study. Molecular compositions of the obtained CHA-G narrow fractions were characterized by FTICR MS. The characteristics of mass spectra are given in Table 2. They include the amount of assigned formulas, the number of CHO and CHON formulas, the calculated intensity-weighted average values of molecular weights, DBE (double bond equivalent), H/C, and O/C ratios.

A consistent decrease in the value of the atomic O/C ratio was observed both with a decrease in polarity and acidity. With a decrease in acidity, a consistent increase in the value of the H/C ratio was also observed, while for the fractions separated by polarity, the value of H/C ratio slightly lowered down to 0.80 up to the fraction CHAG-50, and then increased up to 1.08 observed for CHAG-100. In both sets, the highest values

https://doi.org/10.1021/acsomega.3c08555
ACS Omega 2024, 9, 1858−1869

Table 2. Characterization of FTICR MS Spectra of CHA-G and CHA-G Narrow Fractions

sample name	number of unique formulas[a]	number of CHO formulas	number of CHON formulas	% CHO formulas	% CHON formulas	DBE[b]	H/C[b]	O/C[b]
CHA-G	5652	3976	1676	70.3	29.7	13.9	0.90	0.51
			fractions by polarity					
CHAG 20	3835	2443	1392	63.7	36.3	12.8	0.88	0.48
CHAG 30	4640	2842	1798	61.3	38.7	14.9	0.83	0.46
CHAG 50	5387	3357	2030	62.3	37.7	17.8	0.80	0.47
CHAG 60	5017	2937	2080	58.5	41.5	15.8	0.86	0.42
CHAG 70	4930	3296	1634	66.9	33.1	15.8	0.90	0.40
CHAG 80	4731	3207	1524	67.8	32.2	15.3	0.91	0.38
CHAG 90	4621	3506	1115	75.9	24.1	14.4	0.99	0.34
CHAG 100	5145	4140	1005	80.5	19.5	13.2	1.08	0.31
			fractions by acidity					
CHAG pH8	8035	4962	3073	61.8	38.2	12.9	1.07	0.36
CHAG pH7	5298	3536	1762	66.7	33.3	13.0	1.01	0.38
CHAG pH6	5580	3557	2023	63.7	36.3	12.5	1.01	0.41
CHAG pH5	7372	4408	2964	59.8	40.2	15.3	0.97	0.45
CHAG pH4	5956	3573	2383	60.0	40.0	14.2	0.93	0.48
CHAG pH3	4854	3087	1767	63.6	36.4	14.5	0.89	0.49

[a]Taking into account ^{13}C-isotopologues, compliance with the nitrogen rule, and condition (DBE-O) < 10. [b]Average numerical characteristics.

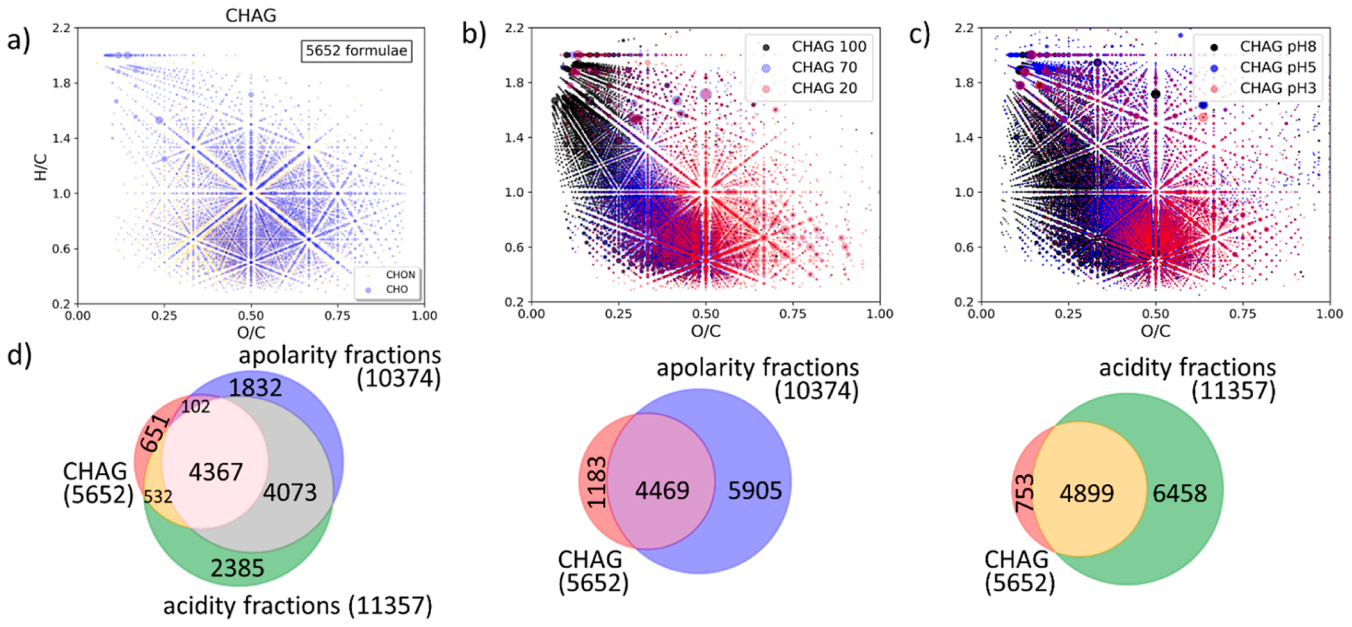

Figure 2. (a–c) Van Krevelen diagrams for: (a) CHAG; (b) CHAG fractions by polarity [CHAG 100 (black), CHAG 70 (blue), and CHAG 20 (red)]; (c) CHAG fractions by acidity [CHAG pH8 (black), pH5 (blue), and pH3 (red)]. Dot sizes in a–c correspond to the relative intensity in mass spectra. (d) Venn diagrams of intersections in molecular composition for CHAG and its fractions. The number of formulas in CHAG and cumulative number of unique formulas in sets of fractions are indicated in brackets.

of DBE were observed for the medium fractions: CHAG-pH5 (15.3) and CHAG-50 (17.8). This is indicative of the higher contribution of aromatic structures. The least polar and least acidic fractions had relatively low average DBE: 12.9 and 13.2 for CHAG-pH8 and CHAG-100, respectively. This is indicative of their predominantly aliphatic nature.

The identified stoichiometries of molecular components of CHAG and its fractions were plotted onto Van Krevelen diagrams (Figures 2a–c and S1 in the Supporting Information). The diagrams show a characteristic shift in molecular compositions of the fractions obtained in this study from highly oxidized aromatic molecules located in the region of hydrolyzable tannins (Figures 2b,c and S1b,o) to less oxidized, hydrophobic structures located both in the region of condensed tannins and lignins, terpenoids and lipids (Figures 2b,c and S1i,j). This trend was observed for both sets of the CHAG fractions.

The undertaken fractionation has brought a 2-fold increase in the number of observed molecular components in the composition of CHA-G (Figure 2d). This could be a result of a less pronounced effect of ionic suppression due to the lesser structural heterogeneity of the fractions compared to the initial humic material.[40,42] Moreover, there were large proportions of molecular components wee observed that were revealed only by fractionation by polarity (1832 formulas) or only by fractionation by acidity (2385 formulas). For both sets of fractions, the common molecular compositions are concentrated in almost the same area of the Van Krevelen diagram

https://doi.org/10.1021/acsomega.3c08555
ACS Omega 2024, 9, 1858−1869

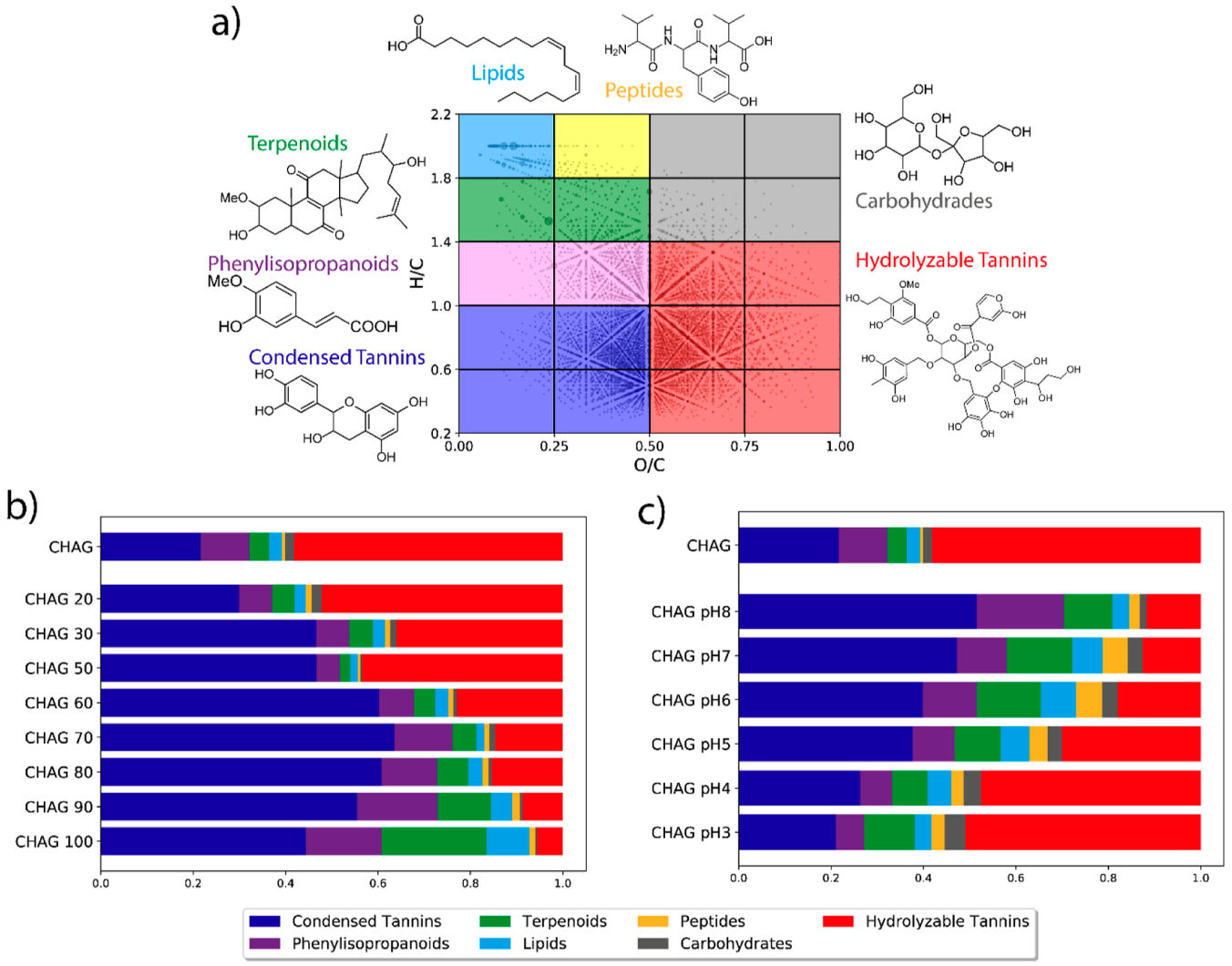

Figure 3. (a) Van Krevelen diagram binned into 20 cells, which are assigned to seven major classes of the biomolecular precursors of HS—condensed tannins, lignins (phenylisopropanoids), terpenoids, other lipids, peptides, carbohydrates, and hydrolyzable tannins (modified from Perminova[43]), (b,c) distribution of the components related to the shown seven chemotypes in the molecular composition of CHA-G and its narrow fractions (b) by polarity; (c) by acidity. The axis *x* corresponds to the contribution of a specific chemotype to the overall intensity of mass spectrum signals. Quantitative data on the contribution of each chemotype (%) are provided in Tables S2 and S3 in the Supporting Information.

(Figure S2): $0.3 \leq O/C \leq 0.6$, $0.3 \leq H/C \leq 1.0$, corresponding to condensed tannins. Thus, for CHA-G, this region turned out to be maximally isomerically saturated and structurally rich because the acidity and polarity of these molecular compositions can vary widely.

Quantitative processing of Van Krevelen diagrams was carried out by chemotyping into 7 regions followed by the calculation of the total signal intensity for each chemotype.[43] The results are shown as horizontal histograms in Figure 3.

There is a decrease in the contribution of hydrolyzed tannins and an increase in the contribution of terpenoid and lignin-like molecular components, with a decrease in both polarity and acidity. However, if the contribution of condensed tannins increases continuously with a decrease in acidity, then with a decrease in polarity it first increases, reaching its maximum at a methanol content of 70 vol %, and then falls, giving way to terpenoids. Figure 3b demonstrates a more significant difference in the molecular composition of fractions during fractionation by acidity.

In general, it can be seen that the major "players" in the molecular ensemble of the narrow fractions of the coal humic acid CHA-G are hydrolyzable and condensed tannins. The different elution or sorption behaviors of the fractions were driven by their ratio.

Biological Activity of the Narrow Fractions of Coal Humic Acid Used in this Study. Biological activity of the narrow fractions of the coal HA used in this study was assessed using two different bioassays: the first one was related to the inhibition of the hydrolytic activity of β-lactamase TEM-1. The second test assessed the antioxidant activity of the fraction. While the first bioassay was indicative of highly specific activity, which is in high demand for developing new β-lactamase inhibitors of nonbeta-lactam nature, the second test characterizes much less specific activity related to the suppression of oxidative stress in living organisms. It was of interest to compare trends in the biological activity of the fractions with regard to these two independent types of activity.

Inhibitory activity against recombinant β-lactamase TEM-1 was measured at fixed concentrations of the enzyme (8 nM) with the use of the chromogenic substrate CENTA[44] (100 μM) and the HS fractions (50 mg/L) as described in the

https://doi.org/10.1021/acsomega.3c08555
ACS Omega 2024, 9, 1858−1869

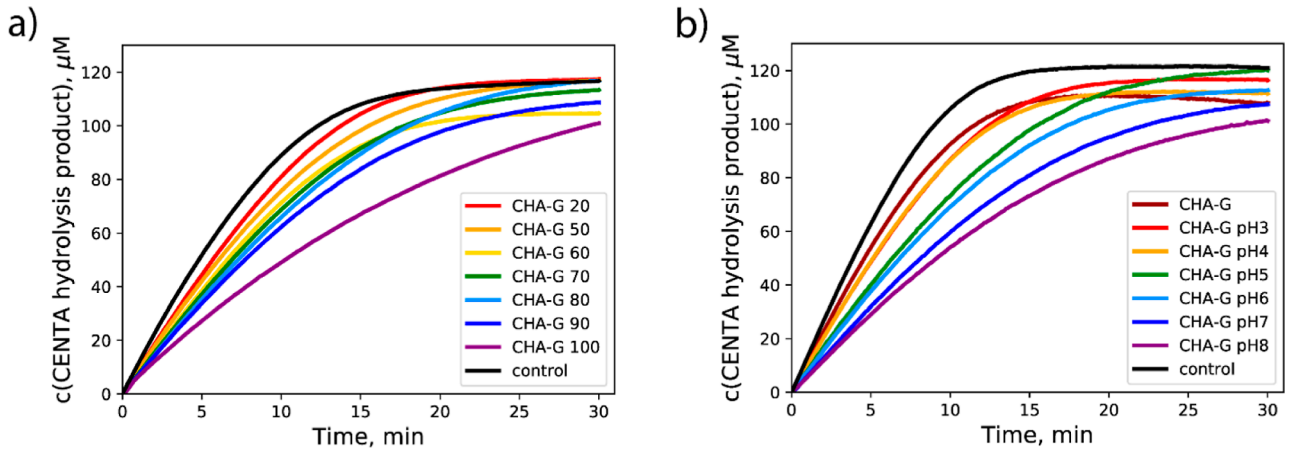

Figure 4. Kinetic curves of CENTA hydrolysis in the presence of CHA-G narrow fractions by (a) polarity and by (b) acidity. Reaction conditions: c(TEM-1) = 8 nM; c(CENTA) = 100 μM; c(HS) = 50 mg/L; 0.05 M PBS, pH 7.0.

Experimental Section. The kinetic curves of the CENTA hydrolysis in the presence of the HS fractions are shown in Figure 4. The relative inhibitory activity (RIA) of each HS fraction was calculated as a relative decrease in the initial rate of the enzymatic reaction in the presence of the HS fraction compared with the control according to eq 2 (Table 3).

Table 3. RIA of CHA-G Narrow Fractions Against β-Lactamase TEM-1[a]

by polarity		by acidity	
fraction	RIA, %	fraction	RIA, %
CHAG 20	18 ± 4[b]	CHAG pH3	22 ± 2
CHAG 50	15 ± 1	CHAG pH4	21 ± 1
CHAG 60	27 ± 1	CHAG pH5	32 ± 1
CHAG 70	29 ± 1	CHAG pH6	40 ± 1
CHAG 80	26 ± 1	**CHAG pH7**	**48±2**
CHAG 90	32 ± 2	**CHAG pH8**	**57±2**
CHAG 100	35 ± 2		

[a]The inhibitory activity of CHA-G was 17 ± 1%. [b]± corresponds to the standard deviation for n = 3.

For both sets of fractions, an increase in the RIA value was observed along with an increase in hydrophobicity and a decrease in acidity of the fraction, respectively. At the same time, a lower acidity value had a more pronounced effect on the ability of HS to inhibit beta-lactamases than an increase in hydrophobicity. This may mean an increase in the relative concentration of inhibitors in the fractions along with a drop in acidity and an increase in hydrophobitiy. It can be assumed that HS contains a number of compounds that differ in chemical compositions and structures and are capable of inhibiting beta-lactamases by different mechanisms. During fractionation, they are segregated into different fractions; their relative concentrations differ; therefore, their RIAs also differ. The CHA-G-pH8 fraction was characterized with the highest RIA value of 57% among both fraction sets. This value of RIA is a factor of 1.6 larger as compared to the most active "polarity" fraction CHA-G 100 (35%) and a factor of 3 larger as compared to the initial CHA-G material (17%). In addition, note that the CHA-G-pH8 fraction is obtained at the first step of the sequential sorption−desorption fractionation. This fact is very advantageous from the point of view of labor and facilities costs while it enables harvesting the most active ingredients at the beginning of the procedure. For the polarity approach, on the contrary, the most active fraction is obtained at the last step of fractionation, which makes it much less attractive.

Antioxidant capacity (AOC) for both sets of the CHAG narrow fractions was measured in relation to the ABTS radical. It was expressed in mmol of antioxidant centers per mg of HS. The obtained value was further recalculated into Trolox equivalent antioxidant capacity (TEAC)—μmol of Trolox equivalent per mg of HS. The kinetic curves of ABTS radical quenching in the presence of CHA-G fractions and the Trolox calibration curves for each experiment are given in the Supporting Information (Figure S3). The obtained results are given in Table 4.

Table 4. TEAC Values for the Narrow Fractions of CHA-G Obtained in this Study

by polarity		by acidity	
fraction	TEAC, μmol/mg	fraction	TEAC, μmol/mg
CHAG 20	6.0 ± 0.1[a]	CHAG pH3	7.2 ± 0.1
CHAG 50	5.3 ± 0.1	CHAG pH4	7.2 ± 0.1
CHAG 60	6.7 ± 0.2	CHAG pH5	6.2 ± 0.1
CHAG 70	5.3 ± 0.2	CHAG pH6	7.4 ± 0.3
CHAG 80	5.5 ± 0.1	**CHAG pH7**	**9.1±0.4**
CHAG 90	6.3 ± 0.5	**CHAG pH8**	**9.1±0.1**
CHAG 100	5.9 ± 0.3		

[a]± is given for the standard deviation (n = 4). The AOC of CHA-G was 7.2 ± 0.2 μmol/mg.

As can be seen from Figure S3 and Table 4, only two HS fractions out of both sets of fractions (CHAG pH7 and CHAG pH8) had AOC values of 9.1 μmol/mg, which were substantially higher than the TEAC of initial CHA-G material of 7.2 μmol/mg. In general, a set of acidity fractions had much higher AOC values compared to polarity fractions. This could be connected to the predominantly oxidized, phenolic nature of fractions isolated with the "acidity" approach. Of importance is that the fractions with the highest AOC (CHAG pH7 and pH8) were also characterized with the highest values of inhibitory activity against β-lactamase TEM-1.

Correlation-Regression Analysis of the Data on Molecular Composition and Biological Activity of the Narrow Fractions of HS Obtained in this Study. The

https://doi.org/10.1021/acsomega.3c08555
ACS Omega 2024, 9, 1858−1869

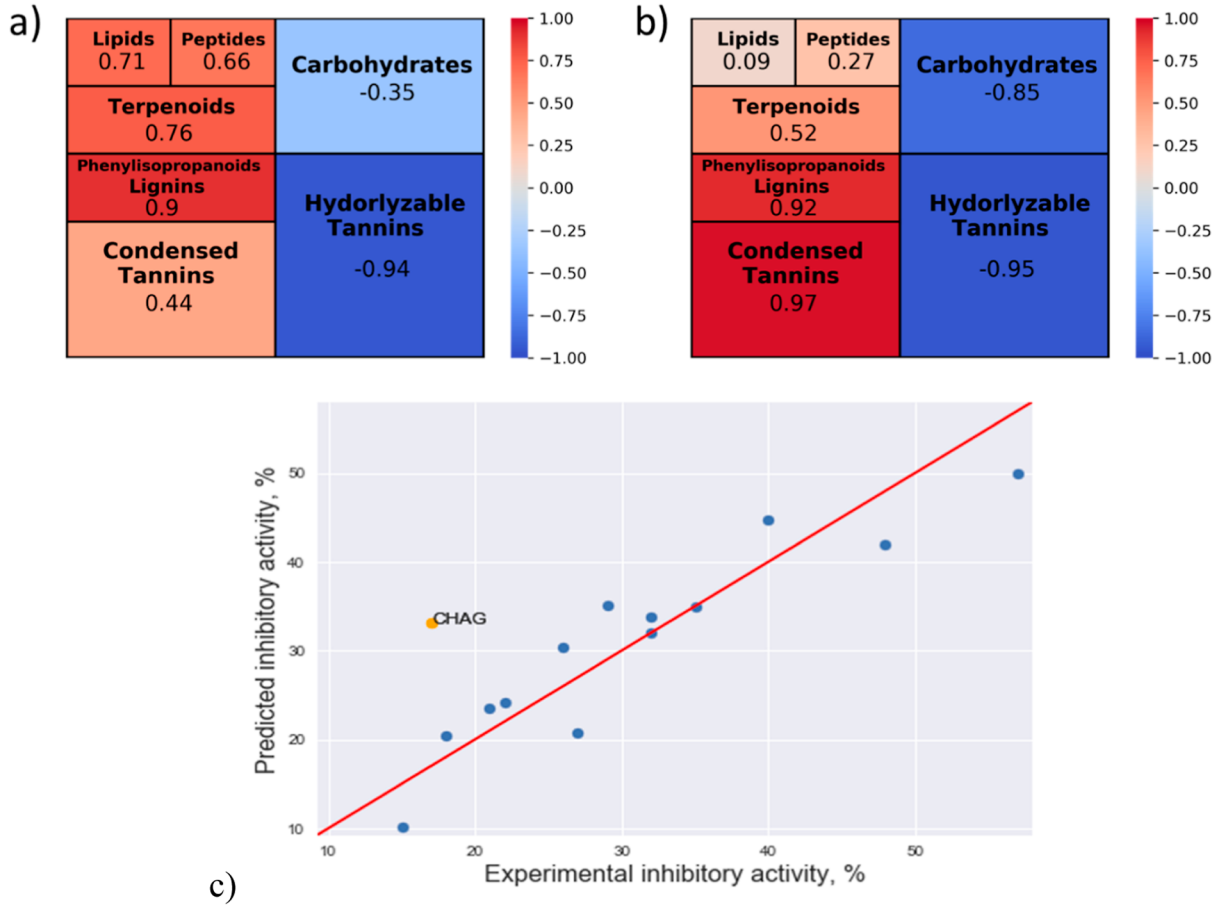

Figure 5. Correlation-regression analysis of the set on structural descriptors of the narrow fractions of CHA-G and their inhibitory activity against β-lactamase TEM-1: (a,b) correlation coefficients between the intensity of the seven chemotypes present in the molecular composition of HS fractions and their inhibitory activity for the set by polarity (SPE-polarity) and acidity (SPE-acidity), respectively (red and blue colors designate positive and negative values of the correlation coefficient, respectively); (c) regression model for predicting inhibitory activity of HS, where narrow fractions of CHA-G are represented by blue dots (training set), and CHA-G is represented by the yellow dot (test set). The best regression model (c) is RIA (%) = 125·D4 + 392·D8 − 12, where D4 and D8 are the normalized intensities of cells 4 and 8 in the Van Krevelen diagram occupied by terpenoids and lignins, respectively.

integral intensities of the main seven chemotypes, normalized to the total spectral intensity, were used as structural descriptors of the HS fractions obtained in this study, whereas inhibitory and antioxidant activities were used as "activity" descriptors for establishing a "structure−activity" relationship for the narrow fractions of CHA-G. The results of the correlation analysis for both sets of fractions are shown in Figures 5 and S4, respectively, with the values of the correlation coefficient (r) shown in the cells with the corresponding chemotype in the Van Krevelen diagrams.

The critical values of the Pearson correlation coefficient r at p = 0.05 and n = 6 and 8 equal to 0.8114 and 0.7067, respectively. As it follows from Figure 5a, for the larger set "by polarity" the significant correlations (r > 0.7067) were observed between inhibitory activity and lignins (0.90), terpenoids (0.76), and hydrolyzable tannins (−0.94). For the smaller set of fractions "by acidity" (Figure 5b), the significant correlations (r > 0.8114) were observed for condensed tannins (0.97) and hydrolyzable tannins (−0.95). It can be noticed that the most substantial contribution into inhibitory activity of the fractions was provided by the hydrophobic moieties (terpenoids, lignins) and, in particular, hydrophobic phenolic moieties in the case of the polarity set (condensed tannins), whereas an increase in the content of hydrophilic hydrolyzable tannins lead to a decrease in inhibitory activity of the narrow fractions of HS.

The united set of the obtained 14 narrow fractions of CHA-G was used for constructing the regression model, which is shown in Figure 5c. It represents one of the best regression models for the prediction of inhibitory activity of HS from the data of FT ICR MS

$$\text{RIA (\%)} = 125 \times \text{D4} + 392 \times \text{D8} - 12 \quad (R^2 = 0.829) \tag{1}$$

where D4 and D8 are normalized intensities of cells 4 and 8 in the Van Krevelen diagram occupied by terpenoids and lignins, respectively, as shown in Figure 3a. The experimental and calculated values for the fractions are shown with blue dots; they represent a training set for the predictive model. The value of inhibitory activity of the parent humic material—CHAG was calculated from the FTICR MS data on its molecular composition using the obtained model. It served as a test point—shown with a yellow dot in Figure 5c. The predicted value agrees well with the experimental value of RIA determined for the parent humic material with the use of bioassay, which is indicative of the reliability of the calculated predictive model (eq 1).

https://doi.org/10.1021/acsomega.3c08555
ACS Omega 2024, 9, 1858−1869

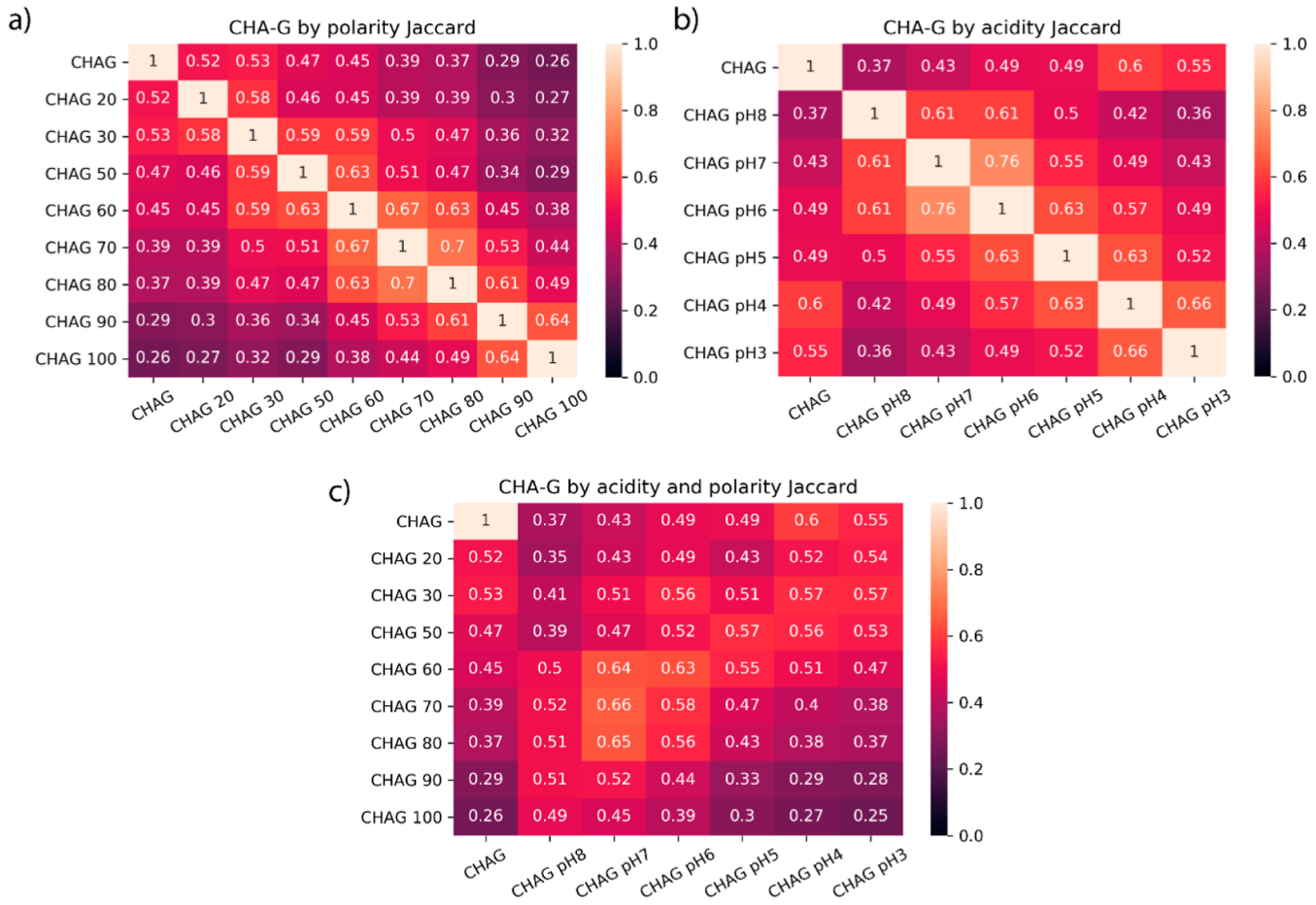

Figure 6. Similarity heatmaps for the two sets of CHA-G fractions based on Jaccard indices: (a) polarity vs polarity, (b) acidity vs acidity, (c) polarity vs acidity. The cell color indicates a portion of common formulas shared by two fractions.

The obtained outcomes of correlation and regression analysis demonstrate a substantial role of hydrophobic low oxidized components such as phenylisopropanoids, condensed tannins, and terpenoids in the inhibitory activity of narrow HS fractions. The values of antioxidant activity (Figure S4) show significant direct correlations only at $p = 0.1$ for the set of acidity fractions with the content of condensed tannins and reverse correlations with the hydrolyzable tannins. This trend is consistent with the reported data on the low oxidized phenols as a source of biological activity of HS.[45] They are also consistent with the relationships discussed above between structure and inhibitory activity of HS. This shows that the narrow HS fractions enriched with condensed tannins, lignins, and terpenoids could be considered as promising sources of biologically active compounds.

Comparison of the Two Fractionation Techniques Used in this Study. We compared the efficacy of the two fractionation techniques used in this study with regard their capability to isolate different chemotypes of the compounds present in the initial humic molecular ensemble. It is important for the targeted isolation of the biologically active compounds. For this purpose, we determined the amount of common molecular formulas in the two sets of fractions and compared them using the Jaccard index.[46] The results are presented as heat maps in Figure 6a–c.

The data show that each pair of the two "neighbor" fractions was characterized by the largest amount of common formulas. The maximum similarity of 76% was observed for a pair of CHA-G pH7 and pH6. The more "distant" fractions were characterized with lesser similarity: a minimum of 27% of common formulas was observed for CHAG 20 and 100. However, in general, it could be concluded that fractionation by polarity yielded less similar fractions compared to the fractionation by acidity. At the same time, fractionation by acidity showed a greater ability to reduce isomeric complexity: the number of common formulas present in all fractions of the SPE-polarity set was a factor of 2 less as compared to the SPE-acidity set (1427 vs 2721). Of additional interest are heat maps of Jaccard similarity coefficients constructed between the two sets of fractions differing in polarity and acidity (Figure 6c). In this case, the two sets shared 47% of common formulas on average. Of particular importance is that the most biologically active fractions from both sets (CHA-G pH7 with CHAG 70 and 80) were the most similar to each other, while the least active fractions were more dissimilar. This could be indicative of the similar chemotypes of the humic structures present in the least polar and the least acidic CHAG fractions, which were responsible for both types of biological activity tested in this study.

It was also of interest to compare van Krevelen diagrams for the two fraction sets under study, which were plotted for the integral values of H/C and O/C calculated for each fraction as intensity averaged values. The corresponding plots are given in Figure 7. The trends in molecular compositions of the two fraction sets of the humic material used in this study—CHA—differed substantially. The linear approximations of the

https://doi.org/10.1021/acsomega.3c08555
ACS Omega 2024, 9, 1858−1869

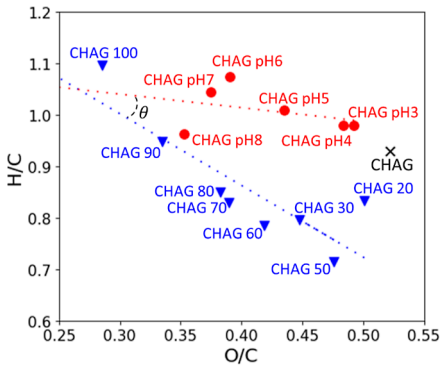

Figure 7. Van Krevelen diagram of the averaged H/C and O/C values of the initial humic material CHAG (black cross) and its SPE fractions arranged by polarity (blue triangles) and by acidity (red circles). Dashed lines represent linear approximations for the two sets of fractions.

obtained trends are shown with dashed lines. The cosine similarity [$\cos(\theta)$] between the linear approximations as vectors in two-dimensional space can serve as an orthogonality measure of the two separation techniques used in this study.[47] If a value of $|\cos(\theta)|$ would equal one (0 or 180° angle), this would represent the highest similarity and complete absence of orthogonality between the two methods as they both impart molecular composition changes in the identical direction. On the contrary, if a value of $\cos(\theta)$ is 0 (90 or −90°), this would signify ideal orthogonality, when the selective isolation of specified molecular compositions could be achieved by employing a combination of these two techniques.

In the case of the techniques used in this study, the cosine similarity value ($\cos(\theta)$) accounted for 0.77 for the two H/C vs O/C relationships calculated for the SPE-polarity and the SPE-acidity (angle of −39.5°). This value suggests that a combination of the two techniques used in our study shows a good promise for a moderate increase in fractionation efficiency as compared to either of the two methods applied alone. Still, the obtained value is far from zero, which is indicative of a burning need for exploration and development of novel fractionation techniques that exhibit much larger orthogonality.

According to the data in Figure 7, it can be concluded that the ratio of O/C of the humic compound has a greater effect on its ability to inhibit beta-lactamase and on its antioxidant activity as compared to the H/C ratio. This follows from the observation that all fractions obtained by fractionation by acidity differed strongly in the O/C value and only slightly—in the H/C value, and these fractions had the most pronounced effect on inhibition. It is important to note that the fractions with maximum RIA differ from the initial humic material CHAG mostly by this parameter. However, it should be noted that the H/C value also had a certain impact on inhibitory activity. Of the fractions separated by polarity, only the most hydrophobic fraction exhibited a greater degree of variation in H/C from the initial material and the highest RIA, which is lower than the highest RIA obtained by decreasing acidity. The strong correlation between the lower O/C ratios and high TEAC values observed in the SPE-acidity set is attributed to the structural characteristics of HS and the chemical selectivity of this fractionation method toward phenols: in HS, the high O/C ratio is attributed to carboxylic groups, and the lower O/C ratio implies fewer carboxylic groups that deactivate the aromatic ring of phenols.

CONCLUSIONS

The conducted research allows us to conclude that the best approach for a one-step separation of biologically active compounds from the coal humic material is an SPE isolation at pH 7−8. Unlike the SPE-polarity approach, which implies sorption of the humic material at pH 2, the portion of irreversibly sorbed components on the cartridge at pH 7−8 is very minute, and the cartridge can be reused for the next extraction. This reduces the labor costs, saves sorbent, and increases the yield of the biologically active fraction of HS material. The separation at pH values >8, as well as the smaller interval in pH values, are promising areas of HS fractionation. Our data, for the first time, demonstrated high biological activity of the fractions obtained by the SPE-acidity approach: the fractions isolated at pH 7 and 8 showed both the highest antioxidant activity as well as inhibitory activity with regard to beta-lactamase TEM-1. Of particular importance is that they were similar in molecular composition to the most hydrophobic fractions isolated with the use of a polarity approach: these fractions also possessed the highest biological activity in the "polarity" set. The obtained results show good promise for the targeted isolation of chemotypes of the given biological activity from the supramolecular ensemble of humic materials. These fractions may serve as new sources for non-β-lactam inhibitors, which are highly sought after by modern medicinal chemistry. The concomitant antioxidant activity is a good prerequisite for developing therapeutic agents of combined action. In addition to nonrenewable geochemical sources of humic materials, suggested approach can be implemented for humic acids extracted from recycled biomass (compost, worms-compost, biochar, biorefinery residues, etc.) or artificial HS that can offer a wider range of promising bioactive components.[48,49] The potential applications of narrow fractions of HS refer both to biomedical technologies and to novel agricultural technologies, in particular, humics-based bioctimulators and nanofertilizers.[50,51] Further research in the field of high-resolution separation of HS materials may bring substantial advances in separation, not only by the chemotypes but by similar chemical scaffolds, which may eventually enable isolation of individual bioactive compounds from the humic supramolecular systems.

EXPERIMENTAL SECTION

Materials. Coal humic acids (CHA-G) were isolated from sodium humate (LLC "Genesis", Russia) by precipitation after acidification with 1 M HCl. High-grade purity conc. HCl and NaOH (Chimmed, Russia) were used for the acidification and dissolution of HS. High-purity deionized water was prepared using a Milli-Q Simplicity 185 water purifying system (Merck, Darmstadt, Germany). pH was measured using a pH meter 713 pH Meter (Metrohm, Switzerland) equipped with a universal glass electrode. HPLC grade methanol (JT Baker, Avantor, Radnor, PA, USA) was used for elution from the SPE cartridges. Hypergrade methanol (for LC−MS LiChrosolv, Merck, Darmstadt, Germany) was used for sample dilution for FT ICR MS analysis. The SPE cartridges were Bond Elut PPL (5.0 g, 60 mL, Agilent Technologies, Waldbronn, Germany). Bond Elut PPL represents a modified copolymer of polystyrene and divinylbenzene. Recombinant β-lactamase TEM-1 was

https://doi.org/10.1021/acsomega.3c08555
ACS Omega 2024, 9, 1858−1869

expressed in *Escherichia coli* and purified as described by Grigorenko et al.[52] Lab-made chromogenic substrate CENTA was used in the inhibitory activity test against β-lactamase. The CENTA was synthesized following the protocol described by Bebrone et al.[44]

SPE Fractionation by Polarity. Fractionation of CHA-G by polarity was carried out according to the approach developed previously in our research group.[16] The SPE cartridge was preactivated by passing 60 mL of methanol and 60 mL of 0.01 M HCl. Five liters of CHA-G solution at a concentration of 70 mg/L were acidified to pH 2 and passed through the cartridge. Acidification was conducted in small portions (70 mL) to avoid precipitation. UV−vis spectra were recorded for CHA-G solutions before and after sorption (pH 2) to estimate the amount of the sorbed material. After the sorption was completed, the cartridge was washed with 120 mL of 0.01 M HCl and dried in an air flow. Then, the sorbed humic material was eluted using H_2O/CH_3OH mixtures with an increasing methanol content. They were passed as fixed volumes of 300 mL at the following water to methanol ratios: 20:80, 30:70, 50:50, 60:40: 70:30, 80:20: 90:10, 100:0. The obtained narrow fractions of the coal humic material used in this study were dried on a rotary evaporator. The obtained samples were assigned the following ciphers: CHAG 20, CHAG 30, CHAG 50, CHAG 60, CHAG 70, CHAG 80, CHAG 90, and CHAG 100 in accordance with the volume content of methanol used for their elution (see mass yields in Table 1).

SPE Fractionation by Acidity. The fractionation of CHA-G by acidity represented a further development of the technique developed previously in our scientific group.[39,40] The SPE cartridge was preactivated by passing 60 mL of methanol. The following describes the procedure for sequential sorption of CHA-G on the cartridge by lowering a pH value of the initial solution to the value x, which corresponded to 8, 7, 6, 5, 4, 3: *acidify* with 1 M HCl to $pH = x$ the CHA-G solution [5 L, initial concentration 100 mg/L, initial pH 11 (adjusted with NaOH), which was passed through the cartridge at the previous stage (or the initial solution of CHA-G in the case of $x = 8$]; *pass 60 mL of water at* $pH = x$ (HCl or NaOH adjusted) through the cartridge (to equilibrate the sorbent); *pass the CHA-G solution at pH x* through the SPE cartridge; *pass 120 mL of 0.01 M HCl solution* through the SPE cartridge (to remove salts); *dry the cartridge* in the air current (≥2 h); *wash off the fraction from the cartridge with methanol* until the optical density of the eluate at the exit of the column approaches zero at λ 254 nm; *repeat* the above steps at the next iteration ($x = x - 1$) for the solution of CHA-G collected after passage through the cartridge. The resulting methanol extracts were dried with a rotary evaporator. The isolated samples were assigned the following ciphers: CHAG pH8, CHAG pH7, CHAG pH6, CHAG pH5, CHAG pH4, CHAG pH3 (see mass yields in Table 1).

FT ICR MS Analysis and Data Processing. Ultrahigh-resolution mass spectra were acquired on a Bruker solariX 15 T FT ICR mass spectrometer (Bruker Daltonics, Bremen, Germany) equipped with a 15 T superconducting magnet and an Apollo II source located at the user facilities of the Zelinski Institute of Organic Chemistry of RAS. The acquisition conditions applied in this study followed those described in refs 37, 53, and 54. The molecular formulas assignments were made using lab-made Transhumus software developed by Anton Grigoriev. The mass accuracy window was set at a value of <0.5 ppm (Da/MDa), and the chemical constraints were used as described in refs 37 and 54. The obtained molecular assignments were used for calculation of H/C and O/C ratios, which were plotted as Van Krevelen diagrams represented by a relationship of H/C versus O/C values as described by Kim et al.[25] The quantitative treatment of the Van Krevelen diagrams was conducted using a cell-partitioning algorithm as described by Perminova.[43] These cells were combined into seven main chemotypes of HS components: condensed tannins, lignins, terpenoids, lipids, peptides, carbohydrates, and hydrolyzable tannins. The obtained values of Van Krevelen diagram occupational densities [for cells (D1−D20) and chemotypes] were further used as quantitative descriptors of the molecular composition.

Study of HS Inhibition Activity with Respect to β-lactamase TEM-1. The study of the inhibition activity of each HS fraction was carried out on a Cary-50 spectrophotometer (Varian, USA) in a 1 cm quartz cuvette. An aliquot of 1311 μL (1386 μL in the case of control reaction without HS) of Na-phosphate buffer solution (PBS) (50 mM, pH 7.0), 75 μL of HS solution (1000 mg/L in PBS) and 14 μL of β-lactamase TEM-1 solution (850 nM in PBS) were mixed in the cuvette. The enzymatic reaction was activated by adding 100 mL of a CENTA solution (1.5 mM in PBS). The total volume of the mixture was 1500 mL. The final concentrations of the reagents were: CENTA—100 μM, β-lactamase TEM-1—8 nM, HS—50 mg/L. The formation of the hydrolysis product was detected at a wavelength of λ 405 nm; each kinetic curve was recorded for 30 min, in two replicates.

The concentration of the CENTA hydrolysis product was calculated using an extinction coefficient of CENTA[44] and an optical density value at λ 405 nm (A_{405}) according to eq 2

$$c\,(\text{CENTA hydrolysis product},\mu M) = (A_{405}/6400) \times 10^6 \quad (2)$$

The initial section of the kinetic curve (3 min) was approximated by a linear function $y = ax + b$, where coefficient a corresponds to the initial rate of the enzymatic reaction, μM/min (v). To calculate RIA, a relative drop in the initial reaction rate was calculated in comparison with the control reaction (without the presence of HS) according to eq 3

$$\text{RIA, \%} = (1 - (v_{\text{inhibitor}}/v_{\text{control}})) \times 100\% \quad (3)$$

where v_{control} and $v_{\text{inhibitor}}$ are the initial rates of the non-inhibited and inhibited reaction, respectively.

Studies on the AOC of the HS Fractions Used in this Study. The AOC of HS in relation to the ABTS radical was evaluated using a FLUOstar Omega microplate reader (BMG LABTECH, Germany). All reactions were carried out in a volume of 250 μL of 0.1 M Na-PBS at pH 7.4. At least a day before the study, a working solution of ABTS radical was prepared: a weight of 11 mg of ABTS was dissolved in 900 μL of water and 100 μL of potassium persulfate solution at a concentration of 20 mg/mL was added. The resulting ABTS radical stock solution (21.4 mM) was left overnight in a dark place. Immediately prior to analysis, the ABTS stock solution was diluted with PBS in a ratio of 1 to 200. ABTS concentration in each well at the initial time was 85.6 μM. This value was used to calculate absorption coefficient of the ABTS radical at λ 734 nm for each measurement. All kinetic curves were represented as a function of a drop in the concentration of the ABTS radical ($\Delta ABTS^{*+}$) versus time. The kinetic curves of ABTS radical quenching in the presence

https://doi.org/10.1021/acsomega.3c08555
ACS Omega 2024, 9, 1858−1869

of HS or Trolox were recorded at a wavelength of λ 734 nm for 40 min (4 replicates). To account for the ABTS radical self-quenching, which is expressed in a small drop in optical density at λ 734 nm without the addition of an antioxidant, a kinetic control curve was subtracted from each kinetic curve for HS. The obtained kinetic curves were approximated by the kinetic model (eq 4)[55]

$$\Delta(\mathrm{ABTS}^{*+}) = \frac{AH_0{}^{*}R^0}{R^0 + K}\left(1 - e^{-k_+[\mathrm{ABTS}^{*+}]\left(1+\frac{K}{R^0}\right)*t}\right) \quad (4)$$

where AH_0 is the initial concentration of the antioxidant, R_0 is the initial ratio $\frac{[\mathrm{ABTS}]}{[\mathrm{ABTS}^{*+}]}$, K is the equilibrium constant, k_+ is the pseudo-first-order velocity constant. $R_0 = 2.5$ for the conditions under which the study was conducted in this work (the ratios of ABTS and $K_2S_2O_8$). The value of AH_0 (μM) obtained as a result of approximation was correlated with the Trolox calibration curve (2, 4, 8, 12, 16, 20 μM) and divided by the concentration of HS (5 mg/L) to obtain the value of TEAC (μmol of Trolox equivalent per mg of HS, μmol/mg).

■ ASSOCIATED CONTENT

Supporting Information

The Supporting Information is available free of charge at https://pubs.acs.org/doi/10.1021/acsomega.3c08555.

Data on elemental and structural group composition of the parent humic material, Van Krevelen diagrams for narrow fractions of CHA-G obtained by different separation techniques, data on the distribution of chemotypes within narrow HS fractions obtained in this study, Van Krevelen diagrams of common formulas between all fractions obtained in this study, kinetic curves for the determination of antioxidant activity of the HS fractions, and correlation diagrams for molecular composition and antioxidant activity (PDF)

■ AUTHOR INFORMATION

Corresponding Author

Irina V. Perminova − *Department of Chemistry, Lomonosov Moscow State University, Moscow 119991, Russia;* orcid.org/0000-0001-9084-7851; Email: iperm@med.chem.msu.ru

Authors

Tatiana A. Mikhnevich − *Department of Chemistry, Lomonosov Moscow State University, Moscow 119991, Russia*

Vitaly G. Grigorenko − *Department of Chemistry, Lomonosov Moscow State University, Moscow 119991, Russia*

Maya Yu. Rubtsova − *Department of Chemistry, Lomonosov Moscow State University, Moscow 119991, Russia;* orcid.org/0000-0003-4025-5967

Gleb D. Rukhovich − *Department of Chemistry, Lomonosov Moscow State University, Moscow 119991, Russia*

Sun Yiming − *Department of Chemistry, Lomonosov Moscow State University, Moscow 119991, Russia*

Anna N. Khreptugova − *Department of Chemistry, Lomonosov Moscow State University, Moscow 119991, Russia;* orcid.org/0000-0003-0521-9135

Kirill V. Zaitsev − *Department of Chemistry, Lomonosov Moscow State University, Moscow 119991, Russia*

Complete contact information is available at: https://pubs.acs.org/10.1021/acsomega.3c08555

Notes

The authors declare no competing financial interest.

■ ACKNOWLEDGMENTS

This work was performed under the financial support of the Russian Science Foundation (Project no. 21-73-20202). We thank Dr. Yulia Ivanova and the Center of Collective Use of the Equipment of the Zelinsky Institute of Organic Chemistry of the Russian Academy of Sciences for recording FT ICR MS spectra.

■ REFERENCES

(1) Stevenson, F. J. *Humus Chemistry: Genesis, Composition, Reactions*; John Wiley & Sons: New York, 1982.

(2) Eshwar, M.; Srilatha, M.; Rekha, K. B.; Sharma, S. H. K. Characterization of Humic Substances by Functional Groups and Spectroscopic Methods. *Int. J. Curr. Microbiol. Appl. Sci.* **2017**, *6* (10), 1768−1774.

(3) Vitiello, G.; Venezia, V.; Verrillo, M.; Nuzzo, A.; Houston, J.; Cimino, S.; D'Errico, G.; Aronne, A.; Paduano, L.; Piccolo, A.; Luciani, G. Hybrid Humic Acid/Titanium Dioxide Nanomaterials as Highly Effective Antimicrobial Agents against Gram(−) Pathogens and Antibiotic Contaminants in Wastewater. *Environ. Res.* **2021**, *193*, 110562.

(4) Van Rensburg, C. E. J.; Van Straten, A.; Dekker, J. An In Vitro Investigation of the Antimicrobial Activity of Oxifulvic Acid. *J. Antimicrob. Chemother.* **2000**, *46*, 853−854.

(5) De Melo, B. A. G.; Motta, F. L.; Santana, M. H. A. Humic Acids: Structural Properties and Multiple Functionalities for Novel Technological Developments. *Mater. Sci. Eng. C* **2016**, *62*, 967−974.

(6) Zhernov, Y. V.; Karamov, E. V.; Perminova, I. V.; Khaitov, M. R.; Khaitov, R. M. Humic Substance-Based Antivirals: Antiretroviral Activity, Mechanisms of Action, and Impact on Mucosal Immunity. *Allergy* **2017**, *72*, 164−165.

(7) Zhernov, Y. V.; Konstantinov, A. I.; Zherebker, A.; Nikolaev, E.; Orlov, A.; Savinykh, M. I.; Kornilaeva, G. V.; Karamov, E. V.; Perminova, I. V. Antiviral Activity of Natural Humic Substances and Shilajit Materials against HIV-1: Relation to Structure. *Environ. Res.* **2021**, *193*, 110312.

(8) Aeschbacher, M.; Graf, C.; Schwarzenbach, R. P.; Sander, M. Antioxidant Properties of Humic Substances. *Environ. Sci. Technol.* **2012**, *46* (9), 4916−4925.

(9) Zykova, M. V.; Schepetkin, I. A.; Belousov, M. V.; Krivoshchekov, S. V.; Logvinova, L. A.; Bratishko, K. A.; Yusubov, M. S.; Romanenko, S. V.; Quinn, M. T. Physicochemical Characterization and Antioxidant Activity of Humic Acids Isolated from Peat of Various Origins. *Molecules* **2018**, *23* (4), 753.

(10) Klein, O. I.; Kulikova, N. A.; Konstantinov, A. I.; Zykova, M. V.; Perminova, I. V. A Systematic Study of the Antioxidant Capacity of Humic Substances against Peroxyl Radicals: Relation to Structure. *Polymers* **2021**, *13* (19), 3262.

(11) Verrillo, M.; Salzano, M.; Savy, D.; Di Meo, V.; Valentini, M.; Cozzolino, V.; Piccolo, A. Antibacterial and Antioxidant Properties of Humic Substances from Composted Agricultural Biomasses. *Chem. Biol. Technol. Agric.* **2022**, *9* (1), 28.

(12) Hobson, C.; Chan, A. N.; Wright, G. D. The Antibiotic Resistome: A Guide for the Discovery of Natural Products as Antimicrobial Agents. *Chem. Rev.* **2021**, *121*, 3464−3494.

(13) Eichenberger, E. M.; Thaden, J. T. Epidemiology and Mechanisms of Resistance of Extensively Drug Resistant Gram-Negative Bacteria. *Antibiotics* **2019**, *8*, 37.

(14) Andersson, D. I.; Balaban, N. Q.; Baquero, F.; Courvalin, P.; Glaser, P.; Gophna, U.; Kishony, R.; Molin, S.; Tønjum, T. Antibiotic Resistance: Turning Evolutionary Principles into Clinical Reality. *FEMS Microbiol. Rev.* **2020**, *44*, 171−188.

(15) Leivers, S. W.; Warn, P. Fulvic Acid and Antibiotic Combination for the Inhibition or Treatment of Multidrug Resistant Bacteria. 20150031767 A1, 2015.
(16) Mikhnevich, T. A.; Vyatkina Turkova, A. V.; Grigorenko, V. G.; Rubtsova, M. Y.; Rukhovich, G. D.; Letarova, M. A.; Kravtsova, D. S.; Vladimirov, S. A.; Orlov, A. A.; Nikolaev, E. N.; Zherebker, A.; Perminova, I. V. Inhibition of Class A β-Lactamase (TEM-1) by Narrow Fractions of Humic Substances. *ACS Omega* **2021**, *6* (37), 23873−23883.
(17) Leyva, D.; Tose, L. V.; Porter, J.; Wolff, J.; Jaffé, R.; Fernandez-Lima, F. Understanding the Structural Complexity of Dissolved Organic Matter: Isomeric Diversity. *Faraday Discuss.* **2019**, *218* (0), 431−440.
(18) Hawkes, J. A.; Patriarca, C.; Sjöberg, P. J. R.; Tranvik, L. J.; Bergquist, J. Extreme Isomeric Complexity of Dissolved Organic Matter Found across Aquatic Environments. *Limnol. Oceanogr. Lett.* **2018**, *3* (2), 21−30.
(19) Ding, Y.; Shi, Z.; Ye, Q.; Liang, Y.; Liu, M.; Dang, Z.; Wang, Y.; Liu, C. Chemodiversity of Soil Dissolved Organic Matter. *Environ. Sci. Technol.* **2020**, *54* (10), 6174−6184.
(20) Gonsior, M.; Valle, J.; Schmitt-Kopplin, P.; Hertkorn, N.; Bastviken, D.; Luek, J.; Harir, M.; Bastos, W.; Enrich-Prast, A. Chemodiversity of Dissolved Organic Matter in the Amazon Basin. *Biogeosciences* **2016**, *13* (14), 4279−4290.
(21) Bae, E.; Na, J. G.; Chung, S. H.; Kim, H. S.; Kim, S. Identification of about 30000 Chemical Components in Shale Oils by Electrospray Ionization (ESI) and Atmospheric Pressure Photoionization (APPI) Coupled with 15 T Fourier Transform Ion Cyclotron Resonance Mass Spectrometry (FT-ICR MS) and a Comparison to Conventional Oil. *Energy Fuels* **2010**, *24*, 2563−2569.
(22) Kujawinski, E. B.; Hatcher, P. G.; Freitas, M. A. High-Resolution Fourier Transform Ion Cyclotron Resonance Mass Spectrometry of Humic and Fulvic Acids: Improvements and Comparisons. *Anal. Chem.* **2002**, *74* (2), 413−419.
(23) Stenson, A. C.; Marshall, A. G.; Cooper, W. T. Exact Masses and Chemical Formulas of Individual Suwannee River Fulvic Acids from Ultrahigh Resolution Electrospray Ionization Fourier Transform Ion Cyclotron Resonance Mass Spectra. *Anal. Chem.* **2003**, *75* (6), 1275−1284.
(24) He, C.; Zhang, Y.; Li, Y.; Zhuo, X.; Li, Y.; Zhang, C.; Shi, Q. In-House Standard Method for Molecular Characterization of Dissolved Organic Matter by FT-ICR Mass Spectrometry. *ACS Omega* **2020**, *5* (20), 11730−11736.
(25) Kim, S.; Kramer, R. W.; Hatcher, P. G. Graphical Method for Analysis of Ultrahigh-Resolution Broadband Mass Spectra of Natural Organic Matter, the Van Krevelen Diagram. *Anal. Chem.* **2003**, *75* (20), 5336−5344.
(26) Rivas-Ubach, A.; Liu, Y.; Bianchi, T. S.; Tolić, N.; Jansson, C.; Paša-Tolić, L. Moving beyond the van Krevelen Diagram: A New Stoichiometric Approach for Compound Classification in Organisms. *Anal. Chem.* **2018**, *90* (10), 6152−6160.
(27) Fedoros, E. I.; Orlov, A. A.; Zherebker, A.; Gubareva, E. A.; Maydin, M. A.; Konstantinov, A. I.; Krasnov, K. A.; Karapetian, R. N.; Izotova, E. I.; Pigarev, S. E.; et al. Novel Water-Soluble Lignin Derivative BP-Cx-1: Identification of Components and Screening of Potential Targets in Silico and In Vitro. *Oncotarget* **2018**, *9* (26), 18578−18593.
(28) Catalá, T. S.; Rossel, P. E.; Álvarez-Gómez, F.; Tebben, J.; Figueroa, F. L.; Dittmar, T. Antioxidant Activity and Phenolic Content of Marine Dissolved Organic Matter and their Relation to Molecular Composition. *Front. Mar. Sci.* **2020**, *7*, 603447.
(29) Monda, H.; McKenna, A. M.; Fountain, R.; Lamar, R. T. Bioactivity of Humic Acids Extracted From Shale Ore: Molecular Characterization and Structure-Activity Relationship with Tomato Plant Yield Under Nutritional Stress. *Front. Plant Sci.* **2021**, *12*, 660224.
(30) Badun, G. A.; Chernysheva, M. G.; Zhernov, Y. V.; Poroshina, A. S.; Smirnov, V. V.; Pigarev, S. E.; Mikhnevich, T. A.; Volkov, D. S.; Perminova, I. V.; Fedoros, E. I. A Use of Tritium-Labeled Peat Fulvic Acids and Polyphenolic Derivatives for Designing Pharmacokinetic Experiments on Mice. *Biomedicines* **2021**, *9* (12), 1787.
(31) Qin, Y.; Zhang, M.; Dai, W.; Xiang, C.; Li, B.; Jia, Q. Antidiarrhoeal Mechanism Study of Fulvic Acids Based on Molecular Weight Fractionation. *Fitoterapia* **2019**, *137*, 104270.
(32) Brown, T. A.; Jackson, B. A.; Bythell, B. J.; Stenson, A. C. Benefits of Multidimensional Fractionation for the Study and Characterization of Natural Organic Matter. *J. Chromatogr. A* **2016**, *1470*, 84−96.
(33) Stenson, A. C.; Ruddy, B. M.; Bythell, B. J. Ion Molecule Reaction H/D Exchange as a Probe for Isomeric Fractionation in Chromatographically Separated Natural Organic Matter. *Int. J. Mass Spectrom.* **2014**, *360* (1), 45−53.
(34) Schepetkin, I. A.; Xie, G.; Jutila, M. A.; Quinn, M. T. Complement-Fixing Activity of Fulvic Acid from Shilajit and Other Natural Sources. *Phytother. Res.* **2009**, *23* (3), 373−384.
(35) Perminova, I. V.; Konstantinov, A. I.; Kunenkov, E. V.; Gaspar, A.; Schmitt-Kopplin, P.; Hertkorn, N.; Kulikova, N. A.; Hatfield, K. Separation Technology as a Powerful Tool for Unfolding Molecular Complexity of Natural Organic Matter and Humic Substances. *Biophysico-Chemical Processes Involving Natural Nonliving Organic Matter in Environmental Systems*; John Wiley & Sons, 2009; pp 487−538..
(36) Dittmar, T.; Koch, B.; Hertkorn, N.; Kattner, G. A Simple and Efficient Method for the Solid-Phase Extraction of Dissolved Organic Matter (SPE-DOM) from Seawater. *Limnol. Oceanogr.: Methods* **2008**, *6* (6), 230−235.
(37) Khreptugova, A. N.; Mikhnevich, T. A.; Molodykh, A. A.; Melnikova, S. V.; Konstantinov, A. I.; Rukhovich, G. D.; Volikov, A. B.; Perminova, I. V. Comparative Studies on Sorption Recovery and Molecular Selectivity of Bondesil PPL versus Bond Elut PPL Sorbents with Regard to Fulvic Acids. *Water* **2021**, *13* (24), 3553.
(38) Lv, J.; Zhang, S.; Luo, L.; Cao, D. Solid-Phase Extraction-Stepwise Elution (SPE-SE) Procedure for Isolation of Dissolved Organic Matter Prior to ESI-FT-ICR-MS Analysis. *Anal. Chim. Acta* **2016**, *948*, 55−61.
(39) Zherebker, A.; Shirshin, E.; Kharybin, O.; Kostyukevich, Y.; Kononikhin, A.; Konstantinov, A. I.; Volkov, D.; Roznyatovsky, V. A.; Grishin, Y. K.; Perminova, I. V.; Nikolaev, E. Separation of Benzoic and Unconjugated Acidic Components of Leonardite Humic Material Using Sequential Solid-Phase Extraction at Different pH Values as Revealed by Fourier Transform Ion Cyclotron Resonance Mass Spectrometry and Correlation Nuclear Magnetic Resonance Spectroscopy. *J. Agric. Food Chem.* **2018**, *66* (46), 12179−12187.
(40) Zherebker, A.; Shirshin, E.; Rubekina, A.; Kharybin, O.; Kononikhin, A.; Kulikova, N. A.; Zaitsev, K. V.; Roznyatovsky, V. A.; Grishin, Y. K.; Perminova, I. V.; Nikolaev, E. N. Optical Properties of Soil Dissolved Organic Matter Are Related to Acidic Functions of Its Components as Revealed by Fractionation, Selective Deuteromethylation, and Ultrahigh Resolution Mass Spectrometry. *Environ. Sci. Technol.* **2020**, *54* (5), 2667−2677.
(41) Zhernov, Y. V.; Kremb, S.; Helfer, M.; Schindler, M.; Harir, M.; Mueller, C.; Hertkorn, N.; Avvakumova, N. P.; Konstantinov, A. I.; Brack-Werner, R.; Schmitt-Kopplin, P.; Perminova, I. V. Supramolecular Combinations of Humic Polyanions as Potent Microbicides with Polymodal Anti-HIV-Activities. *New J. Chem.* **2017**, *41* (1), 212−224.
(42) Rodgers, R. P.; Mapolelo, M. M.; Robbins, W. K.; Chacón-Patiño, M. L.; Putman, J. C.; Niles, S. F.; Rowland, S. M.; Marshall, A. G. Combating Selective Ionization in the High Resolution Mass Spectral Characterization of Complex Mixtures. *Faraday Discuss.* **2019**, *218*, 29−51.
(43) Perminova, I. V. From Green Chemistry and Nature-like Technologies towards Ecoadaptive Chemistry and Technology. *PAC* **2019**, *91*, 851−864.
(44) Bebrone, C.; Moali, C.; Mahy, F.; Rival, S.; Docquier, J. D.; Rossolini, G. M.; Fastrez, J.; Pratt, R. F.; Frère, J. M.; Galleni, M. CENTA as a Chromogenic Substrate for Studying β-Lactamases. *Antimicrob. Agents Chemother.* **2001**, *45* (6), 1868−1871.

https://doi.org/10.1021/acsomega.3c08555
ACS Omega 2024, 9, 1858−1869

(45) Yoon, H. Y.; Jeong, H. J.; Cha, J.-Y.; Choi, M.; Jang, K.-S.; Kim, W. Y.; Kim, M. G.; Jeon, J.-R. Structural Variation of Humic-like Substances and its Impact on Plant Stimulation: Implication for Structure-Function Relationship of Soil Organic Matters. *Sci. Total Environ.* **2020**, *725*, 138409.
(46) Longnecker, K.; Futrelle, J.; Coburn, E.; Kido Soule, M. C.; Kujawinski, E. B. Environmental Metabolomics: Databases and Tools for Data Analysis. *Mar. Chem.* **2015**, *177*, 366−373.
(47) Sidorov, G.; Gelbukh, A.; Gómez-Adorno, H.; Pinto, D. Soft Similarity and Soft Cosine Measure: Similarity of Features in Vector Space Model. *Comput. Sist.* **2014**, *18* (3), 491−504.
(48) Yang, F.; Fu, Q.; Antonietti, M. Anthropogenic, Carbon-Reinforced Soil as a Living Engineered Material. *Chem. Rev.* **2023**, *123*, 2420−2435.
(49) Rehman, J. U.; Joe, E.-N.; Yoon, H. Y.; Kwon, S.; Oh, M. S.; Son, E. J.; Jang, K.-S.; Jeon, J.-R. Lignin Metabolism by Selected Fungi and Microbial Consortia for Plant Stimulation: Implications for Biologically Active Humus Genesis. *Microbiol. Spectrum* **2022**, *10* (6), No. e0263722.
(50) Jeong, H. J.; Oh, M. S.; Rehman, J. U.; Yoon, H. Y.; Kim, J.-H.; Shin, J.; Shin, S. G.; Bae, H.; Jeon, J.-R. Effects of Microbes from Coal-Related Commercial Humic Substances on Hydroponic Crop Cultivation: A Microbiological View for Agronomical Use of Humic Substances. *J. Agric. Food Chem.* **2021**, *69* (2), 805−814.
(51) Yoon, H. Y.; Lee, J. G.; Esposti, L. D.; Iafisco, M.; Kim, P. J.; Shin, S. G.; Jeon, J.-R.; Adamiano, A. Synergistic Release of Crop Nutrients and Stimulants from Hydroxyapatite Nanoparticles Functionalized with Humic Substances: Toward a Multifunctional Nanofertilizer. *ACS Omega* **2020**, *5* (12), 6598−6610.
(52) Grigorenko, V. G.; Andreeva, I. P.; Rubtsova, M. Y.; Deygen, I. M.; Antipin, R. L.; Majouga, A. G.; Egorov, A. M.; Beshnova, D. A.; Kallio, J.; Hackenberg, C.; Lamzin, V. S. Novel Non-β-Lactam Inhibitor of β-Lactamase TEM-171 Based on Acylated Phenoxyaniline. *Biochimie* **2017**, *132*, 45−53.
(53) Mueller, C.; Kremb, S.; Gonsior, M.; Brack-Werner, R.; Voolstra, C. R.; Schmitt-Kopplin, P. Advanced Identification of Global Bioactivity Hotspots via Screening of the Metabolic Fingerprint of Entire Ecosystems. *Sci. Rep.* **2020**, *10* (1), 1319.
(54) Koch, B. P.; Dittmar, T.; Witt, M.; Kattner, G. Fundamentals of Molecular Formula Assignment to Ultrahigh Resolution Mass Data of Natural Organic Matter. *Anal. Chem.* **2007**, *79* (4), 1758−1763.
(55) Klein, O. I.; Kulikova, N. A.; Filimonov, I. S.; Koroleva, O. V.; Konstantinov, A. I. Long-Term Kinetics Study and Quantitative Characterization of the Antioxidant Capacities of Humic and Humic-like Substances. *J. Soils Sediments* **2018**, *18* (4), 1355−1364.

https://doi.org/10.1021/acsomega.3c08555
ACS Omega 2024, 9, 1858−1869